Radiology

Normal and Altered Three-dimensional Portal Venous Hemodynamics in Patients with Liver Cirrhosis[1]

Zoran Stankovic, MD
Zoltan Csatari, MD
Peter Deibert, MD
Wulf Euringer, MD
Philipp Blanke, MD
Wolfgang Kreisel, MD
Zahra Abdullah Zadeh, MD
Felix Kallfass, MD
Mathias Langer, MD
Michael Markl, PhD

Purpose: To compare time-resolved three-dimensional (3D) phase-contrast magnetic resonance (MR) imaging with three-directional velocity encoding (flow-sensitive four-dimensional [4D] MR imaging), with Doppler ultrasonography (US) as standard of reference, for investigating alterations in 3D portal venous hemodynamics in patients with liver cirrhosis compared with healthy age-matched control subjects and healthy young volunteers.

Material & Methods: This prospective study was approved by the local ethics committee, and written informed consent was obtained from all participants. Three-dimensional portal venous hemodynamics was assessed, employing flow-sensitive 4D MR imaging with a 3-T MR system (spatial resolution, approximately 2 mm^3; temporal resolution, approximately 45 msec) in 20 patients with hepatic cirrhosis, 20 healthy age-matched control subjects, and 21 healthy young volunteers. Flow characteristics were analyzed by using 3D streamlines and time-resolved particle traces. Quantitative analyses were performed by retrospectively evaluating regional peak and mean velocities, flow volume, and vessel area. Doppler US was used as standard of reference. Independent-sample *t* tests or Wilcoxon-Mann-Whitney tests were applied for comparing each subject group. Paired-sample *t* tests or Wilcoxon tests were applied when comparing MR imaging and US.

Results: Three-dimensional visualization of portal venous hemodynamics was successful, with complete visualization of the vessels in 18 patients and 35 volunteers, with limitations in the left intrahepatic branches (87%, reader A; 89%, reader B). A moderate but significant correlation was observed between 4D MR imaging and Doppler US in nearly all maximum and mean velocities, flow volumes, and vessel areas (r = 0.24–0.64, P = .001–.044). With MR imaging, significant underestimation was observed of intrahepatic flow velocities and flow volumes, except vessel area, which Doppler US represented as even lower ($P < .001$ to P = .045). Six patients had collateralization with reopened umbilical vein, while one had flow reversal in the superior mesenteric vein visible at MR imaging only.

Conclusion: Flow-sensitive 4D MR imaging may constitute a promising, alternative technique to Doppler US for evaluating hemodynamics in the portal venous system of patients with liver cirrhosis and may be a means of assessing pathologic changes in flow characteristics.

[1] From the Department of Diagnostic Radiology and Medical Physics (Z.S., Z.C., W.E., P.B., Z.A.Z., F.K., M.L.) and Department of Gastroenterology (P.D., W.K.), University Medical Center Freiburg, Hugstetter Strasse 55, 79106 Freiburg, Germany; and Departments of Radiology and Biomedical Engineering, Northwestern University, Chicago, Ill (M.M.). Received January 19, 2011; revision requested March 3; final revision received July 25; accepted September 9; final version accepted October 27. **Address correspondence to** Z.S. (e-mail: *zoran.stankovic@uniklinik-freiburg.de*).

Patients with progressive liver cirrhosis typically develop a hyperdynamic syndrome with increasing cardiac output and heart rate, resulting in increased splanchnic inflow (1). This systemic reaction is associated with lower blood pressure and systemic vascular resistance. Because of growing sinusoidal resistance, portal flow volume and flow velocity in patients with liver cirrhosis are reduced, while hepatic resistance and portal vein pressure rise, promoting the formation of portosystemic collateral vessels (2). The decrease in portal flow volume is, to some extent, balanced by the hepatic arterial buffer response, which acts as an intrinsic regulatory system (3). Invasive and noninvasive methods are used for monitoring complications related to portal hypertension and the response to pharmacologic treatment (4,5).

Advances in Knowledge

- Flow-sensitive four-dimensional (4D) MR imaging can help evaluate three-dimensional portal venous blood flow in patients with liver cirrhosis and in control groups, with good image quality (complete visualization of the vessels in 18 patients with cirrhosis and 35 healthy age-matched control subjects and healthy young volunteers) and low observer variability (Cohen κ coefficient of 0.70).
- Complex vascular hemodynamics of the portal venous system of patients with liver cirrhosis can be visualized, depicting abnormal flow patterns in six patients (eg, reopening of the umbilical vein or flow reversal in the superior mesenteric vein which was only visible with MR imaging).
- Quantitative flow analysis revealed moderate but significant correlation for regional hemodynamic parameters (including maximum and mean velocities, flow volume, and vessel area) between 4D MR imaging and the reference standard Doppler US (r = 0.24–0.64, P = .001–.044).

Doppler ultrasonography (US) is the current noninvasive clinical standard for identifying and assessing hemodynamic changes in portal venous flow in patients with hepatic disease, such as liver cirrhosis and portal hypertension. Researchers in US studies have demonstrated a significant correlation between main portal vein flow volume and mean velocity and the liver cirrhosis stage (6,7). Nevertheless, the diagnostic value of Doppler US is limited, as a result of interobserver dependency and variability in the actual portal blood flow velocity values caused by measurement errors or poor examination conditions when taking Doppler measurements. However, portal blood flow may not always be fully visible at US, resulting in an incomplete or inaccurate evaluation of blood flow in the peripheral branches of the portal vein (8).

An alternative technique for evaluating portal venous hemodynamics and the severity of chronic liver disease is computed tomography (9,10). However, this technique is limited by radiation exposure and side effects of the intravenous iodinated contrast media, such as nephrotoxicity and allergic reactions (11,12).

Magnetic Resonance (MR) imaging is the widespread imaging modality of choice for following patients with liver cirrhosis to assess the hepatic vasculature, to grade the severity of fibrosis, and to detect hepatocellular carcinomas (13–16). Researchers in several studies have correlated splanchnic blood flow changes with cirrhosis stages by using contrast material–enhanced MR perfusion (13), contrast-enhanced MR angiography (14), and nonenhanced techniques (15,16).

Implication for Patient Care

- Flow-sensitive 4D MR imaging may constitute an alternative to Doppler US as a noninvasive technique, providing information on morphologic characteristics and portal venous hemodynamics in patients with liver cirrhosis.

However, these MR imaging techniques are limited by incomplete coverage of the portal venous system, susceptibility to breathing artifacts, and incomplete visualization of blood flow in peripheral branches. Flow-sensitive four-dimensional (4D) MR imaging may constitute an alternative by offering full volumetric (three-dimensional [3D] imaging) and functional (encoding of all three blood flow velocity directions) coverage of the vascular region of interest. Previous applications focused on the arterial system, successfully allowing evaluation of normal and pathologic 3D hemodynamics in vascular territories, such as the aorta, the heart, the intracranial blood vessels, and the carotid arteries (17–20).

The feasibility of flow-sensitive 4D MR imaging for evaluating 3D portal venous flow was reported recently (21,22). The aim of this study was to compare flow-sensitive 4D MR imaging with Doppler US for investigating alterations in 3D portal venous hemodynamics in patients with liver cirrhosis compared with healthy age-matched control subjects and healthy young volunteers.

Published online
10.1148/radiol.11110127 **Content code:** GI

Radiology 2012; 262:862–873

Abbreviations:
4D = four-dimensional
MELD = model for end-stage liver disease
3D = three-dimensional

Author contributions:
Guarantors of integrity of entire study, Z.S., F.K., M.M.; study concepts/study design or data acquisition or data analysis/interpretation, all authors; manuscript drafting or manuscript revision for important intellectual content, all authors; approval of final version of submitted manuscript, all authors; literature research, Z.S., P.D., W.K., Z.A.Z., M.M.; clinical studies, Z.S., Z.C., P.D., W.E., W.K., Z.A.Z., F.K., M.M.; statistical analysis, Z.S., Z.C., P.B., Z.A.Z.; and manuscript editing, Z.S., Z.C., P.D., W.E., P.B., W.K., Z.A.Z., M.L., M.M.

Potential conflicts of interest are listed at the end of this article.

Materials and Methods

Study Population

This prospective study was approved by our local ethics committee, and written informed consent was obtained from all participants.

Between February 2009 and March 2010, 1850 patients were referred to our Division of Gastroenterology for medical treatment. Patients were included in the study if they had liver cirrhosis, as proved by histologic examination or by Doppler US and serologic testing. They had to undergo a Doppler US examination for clinical care for possible enrollment in the study; afterward, US was repeated as part of the study. Patients were excluded if there was a history of known malignant liver tumor, contraindication to MR imaging examination, or the absence of informed consent. Seven hundred thirty-four patients had liver cirrhosis proved by histologic examination or Doppler US and serologic testing. Seven hundred fourteen patients were excluded: 602 patients did not undergo a Doppler US examination, 18 patients had liver carcinoma or metastases, seven patients had a heart valve prosthesis or pacemaker, and 87 patients declined to participate in the study. Twenty patients with cirrhosis (mean age, 57.7 years ± 11.6 [standard deviation]; range, 27–73 years) were included in the study; 12 were male patients (mean age, 58.1 years ± 11.1; range, 42–73 years), and eight were female patients (mean age, 57.0 years ± 13.1; range, 27–73 years). Liver cirrhosis was histologically confirmed in eight patients and was confirmed with Doppler US and serologic testing in 12 patients. For patients with a known history of liver cirrhosis, we used the Child-Pugh score to evaluate the degree of liver failure (23). Of the 20 patients with cirrhosis, 16 had Child-Pugh score A for liver cirrhosis, three had Child-Pugh score B, and one had Child-Pugh score C (Table 1). Causes of cirrhosis were alcohol abuse (n = 6), primary biliary cirrhosis (n = 4), chronic viral hepatitis (n = 3), autoimmune cirrhosis (n = 2), unknown or idiopathic disease (n = 5) . We also included 20 healthy age-matched control subjects (mean age, 58.6 years ± 5.9; range, 50–69 years); 10 were male patients (mean age, 59.3 years ± 6.1; range, 50–69 years) and 10 were female patients (mean age, 57.8 years ± 5.8; range, 52–68 years). In addition, we included 21 healthy young volunteers (mean age, 27.5 years ± 3.3; range, 22–37 years); seven were male patients (mean age, 29.4 years ± 1.6; range, 27–31 years), and 14 were female patients (mean age, 26.6 years ± 3.6; range, 22–37 years) (Table 1). Healthy age-matched control subjects and healthy young volunteers were without any known medical history or clinical signs of liver cirrhosis. All measurements were taken after overnight fasting.

MR Imaging

For time-resolved 3D assessment of portal venous hemodynamics, we used a 3D time-resolved (cine) radiofrequency-spoiled phase-contrast gradient-echo sequence with three-directional velocity encoding (also termed flow-sensitive 4D MR imaging) at a 3-T MR system (Magnetom Trio; Siemens, Erlangen, Germany), with a maximum gradient strength of 40 mT/m and a minimum rise time of 200 μsec (24). The receive system consisted of a flexible six-element chest coil and a six-element spine coil. Prospective electrocardiographic gating (cine imaging) and k-space segmented data acquisition, with N_k = two phase-encoding lines per time frame, were performed to synchronize data acquisition with the cardiac cycle. Imaging was performed during free breathing by using navigator gating of the spleen-lung interface and data acquisition during an end-expiratory acceptance window of 7 mm, as described previously (24). Velocity encoding was obtained by successively executing one reference and three velocity-sensitive images (repetition time msec/echo time msec, 5.6/3.0), resulting in a temporal resolution of 4 N_k, with repetition time of 44.8 msec and a measured spatial resolution of 1.6 × 2.1 × 2.4 mm^3. Velocity-encoding sensitivity was 50 cm/sec for all three flow-encoding directions. Data were acquired at an axial oblique 3D volume angled along the portal vein and adapted to each individual's anatomy. Further parameters were as follows: field of view, 220 × 320 mm^2; imaging matrix, 192 × 152; flip angle, α = 7°; 36 sections per slab; bandwidth, 450 Hz/pixel; partial echo readout (echo maximum after 30% of readout gradient); parallel imaging (generalized autocalibrating partially parallel acquisitions) with reduction factor of two and 32 reference lines.

Data Analysis

The flow-sensitive 4D MR imaging data were postprocessed by using a homebuilt analysis tool (Matlab; MathWorks, Natick, Mass), including noise filtering, correction for eddy currents (25) and Maxwell terms (26), as well as velocity antialiasing (27). A 3D phase-contrast MR angiogram was derived from the flow-sensitive 4D MR imaging data, as described previously (28). The 3D phase-contrast MR angiogram was used to depict portal venous vascular geometry by using isosurface rendering (EnSight; CEI, Apex, NC).

Five analysis planes were manually placed by a radiology resident (F.K.) in the portal venous system in the splenic and superior mesenteric veins, splenic-mesenteric confluence, and right and left intrahepatic portal vein branches prior to image evaluation by reviewers (Fig 1). For qualitative analysis, time-resolved 3D particle traces (virtual particles representing the dynamics of 3D blood flow over the cardiac cycle) and 3D streamlines (3D traces tracking the spatial distribution of the 3D velocities measured for each cardiac time frame) originating from the five analysis planes were used for 3D flow visualization (17). All data sets were evaluated by using 3D viewing software (EnLiten; CEI). The software allowed interactive inspection and rotation of the streamlines and time-resolved particle traces from any view angle.

Demographics were analyzed for each subject group (patients with cirrhosis, healthy age-matched control subjects, and healthy young volunteers), including age, sex, body weight, height, heart rate, blood pressure before and after examination, total flow acquisition time, and number of acquired cardiac time frames over

Table 1

Demographics for All Three Cohorts and Clinical Parameters in Patients with Liver Cirrhosis

A: Clinical Data for Groups A–C

Demographic Characteristics	Group A	Group B	Group C
Age (y)	57.7 ± 11.6	58.6 ± 5.9	27.5 ± 3.3*
Sex			
No. female	8	10	14
No. male	12	10	7
Body weight (kg)	75.8 ± 14.7	73.3 ± 11.7	67.9 ± 11.3*
Height (cm)	173.8 ± 9.3	172.4 ± 10.0	173.7 ± 8.3
Heart rate (beats/min)	71.3 ± 11.7	66.9 ± 9.6	61.8 ± 9.7*
Blood pressure (mm Hg)			
Before examination	135/84 ± 18/10	131/86 ± 15/8	120/80 ± 11/7*
After examination	132/83 ± 15/12	128/85 ± 12/8	122/82 ± 11/9*
Total flow acquisition time (min)	14.6 ± 7.3	18.1 ± 7.5	21.9 ± 8.6*
Intervals†	16.7 ± 2.9	17.3 ± 2.7	19.6 ± 3.1

B: Clinical Parameters for Group A Only

Laboratory Tests	Child-Pugh Class A (*n* =16)	Child-Pugh Class B (*n* =3)	Child-Pugh Class C (*n* = 1)
MELD score	8.1 ± 2.2	13.7 ± 4.1	26
Total serum bilirubin level (mg/dL)	1.0 ± 0.5	1.7 ± 0.6	11.9
Serum albumin level (g/dL)	4.2 ± 0.4	2.7 ± 0.6	4.0
International normalized ratio	1.1 ± 0.1	1.3 ± 0.3	1.6
No. patients with ascites	2	3	1
No. of patients with hepatic encephalopathy	0	0	1
Serum creatinine level	1.0 ± 0.1	1.4 ± 0.3	1.8

Note.—Group A = patients with cirrhosis, group B = healthy age-matched control subjects, group C = healthy young volunteers, and MELD = model for end-stage liver disease. Data are the mean ± standard deviation except where otherwise specified. To convert to Système International units for total serum bilirubin level in micromoles per liter, multiply by 17.104, for serum albumin level in grams per liter, multiply by 10, and for serum creatinine level in micromoles per liter, multiply by 88.4.

* Significant difference for age, body weight, heart rate, and blood pressure before and after examination between healthy young volunteers versus patients with cirrhosis and healthy age-matched control subjects and for flow examination time between patients with cirrhosis and healthy young volunteers.

† Intervals = number of acquired cardiac time frames over the cardiac cycle.

the cardiac cycle. Furthermore, we assessed the clinical parameters of the patients with cirrhosis by comparing Child-Pugh classification, MELD score, total serum bilirubin level, serum albumin level, international normalized ratio, ascites, hepatic encephalopathy, and serum creatinine level. The 4D MR imaging and Doppler US measurements were subjected to complementary subanalysis of quantitative measurements and MELD scores, including maximum and mean velocities, flow volume, and area.

Two independent readers (Z.S., a radiologist with 6 years of MR imaging experience; Z.C., a 3rd-year radiology resident) evaluated streamlines and time-resolved particle traces in all 61 subjects according to the vessel-visualization criteria (score 0, not visible; score 1, partially visible; score 2, completely visible) and leakage, which defines the existence of 3D streamlines leaving the vessel lumen caused by partial volume effects (ie, close proximity of neighboring vessels [present or absent]). An overall consensus of identical findings for both readers was calculated. Readers were blinded to patient-identifying information and the presence of cirrhosis.

We also analyzed the extrahepatic and intrahepatic portal vein flow patterns of the 20 patients with liver cirrhosis on the basis of 4D MR imaging findings with the same two readers previously described and on the basis of Doppler US findings, with one other reader (P.D., a board-certified gastroenterologist with more than 20 years of experience in performing Doppler US) to evaluate modifications in portal vein hemodynamics (eg, reopening of the umbilical vein, retrograde blood flow or vortex flow in the splenic-mesenteric confluence). Both measurements were performed within an interval of 3 hours between the examinations. We also quantitatively analyzed portal venous blood flow velocities retrospectively by using a homebuilt tool (Matlab; MathWorks) on the basis of the five analysis planes. Data were exported into the evaluation software, which was used to manually delineate the vessel lumen boundaries for each cardiac time frame. Blood flow velocities were quantified by one reader (Z.C.) for all measurements in patients with cirrhosis, healthy age-matched control subjects, and healthy young volunteers. Maximum and mean velocities, flow volume, and vessel lumen area were calculated in all patients with cirrhosis, healthy age-matched control subjects, and healthy young volunteers.

Doppler US

Doppler US was performed by the same gastroenterologist as mentioned above. Patients with cirrhosis, healthy age-matched control subjects, and healthy volunteers were examined in the supine position during breath holding. A 3.5-MHz convex-array transducer (Toshiba Aplio XV; Toshiba Europe, Neuss, Germany) was applied at an insonation angle smaller than 60°. The Doppler windows corresponded to the preassigned five emitter planes from 4D MR imaging. Maximum and mean velocities, flow volumes, and vessel lumen areas represent the mean of three measurements.

Statistical Analysis

All statistical analyses were performed by using commercially available software (SPSS 16.0; SPSS, Chicago, Ill).

Figure 1

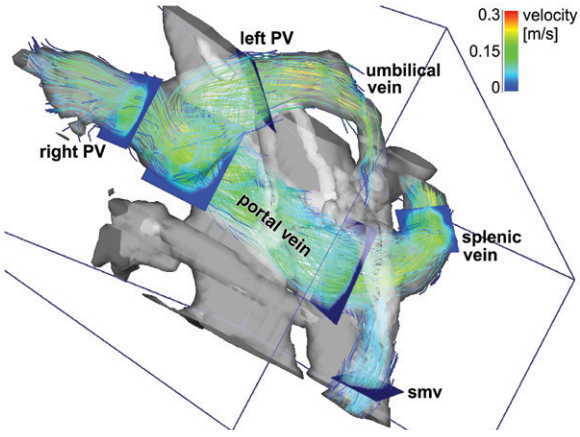

Figure 1: Portal venous system visualized by using streamlines in a 60-year-old female patient with liver cirrhosis (Child-Pugh class A). Emitter planes (in blue) were positioned in the splenic vein and superior mesenteric vein *(smv)*, splenic-mesenteric confluence, and right intrahepatic portal vein branch *(right PV)* and left intrahepatic portal vein branch *(left PV)*. The gray isosurface 3D phase-contrast MR angiogram was calculated from flow-sensitive 4D MR imaging data. Streamlines depict physiologic flow in the extrahepatic portal venous system with inflow in the splenic-mesenteric confluence from the splenic and superior mesenteric veins. Flow over the left branch of the intrahepatic portal vein into a recanalized umbilical vein is visible. These findings were confirmed with the clinical standard Doppler US.

Table 2

Summary of Results of 3D Flow Visualization in All Three Cohorts for Readers A and B

Structure or Feature	Visualization for Reader A	Visualization for Reader B	Overall
Superior mesenteric vein	100	100	100
Splenic vein	98 (60/61)	100	99 (60.5/61)
Splenic-mesenteric confluence	100	100	100
Right portal vein branch	100	100	100
Left portal vein branch	87 (53/61)	89 (54/61)	88 (53.5/61)
Streamlines leakage present	84 (51/61)	85 (52/61)	84 (51.5/61)
Particle traces leakage present	51 (31/61)	48 (29/61)	49 (30/61)

Note.—Data are percentages. Numbers in parentheses are no. of data sets with visualization score of 2 (completely visible) divided by total no. from all three data sets and were used to calculate the percentages. Percentages were rounded. Reader A = Z.S. Reader B = Z.C.

Cohen κ statistics were performed to evaluate observer agreement in the qualitative visualization of streamlines and particle traces. The κ values of 0.21–0.40 represented fair agreement, those of 0.41–0.60 represented moderate agreement, those of 0.61–0.80 represented substantial agreement, and those of 0.81–1.00 represented excellent agreement (29).

To test for significant differences in nominal scale data, the χ^2 test and Fisher exact test were used. Separate tests were conducted for each of the five specific anatomic regions of the portal venous system for different subject groups and different imaging modalities.

Independent-sample *t* tests or Mann-Whitney tests were applied to compare the subject groups (patients with cirrhosis, healthy age-matched control subjects, and healthy young volunteers), while we based the comparison of MR imaging and Doppler US imaging modalities on paired-sample *t* tests or Wilcoxon tests. The Gaussian distribution was assessed via the Kolmogorov-Smirnov test. When the hypothesis of a Gaussian distribution was not rejected, *t* tests were performed. Otherwise, Mann-Whitney tests (subject group comparison) or Wilcoxon tests (imaging modality comparison) were used. Correlation between MR imaging and Doppler US was assessed with the Spearman correlation procedure. A *P* value of less than .05 was considered indicative of a significant difference.

Results

Demographics for all three groups included in this study are summarized in Tables 1 and 2. Flow-sensitive 4D MR imaging of portal venous hemodynamics was successful in all 20 patients with cirrhosis (mean total flow acquisition time, 14.6 minutes ± 7.3), 20 healthy age-matched control subjects (mean total flow acquisition time, 18.1 minutes ± 7.5), and 21 healthy young volunteers (mean total flow acquisition time, 21.9 minutes ± 8.6). Flow-sensitive 4D MR imaging was acquired with prospective electrocardiographic gating and during free breathing by using navigator gating that was based on the respiration-induced motion of the spleen-lung interface. Since patients with cirrhosis had higher heart rates than did the healthy age-matched control subjects and the healthy young volunteers (Table 1), the examination times for patients with cirrhosis were shorter. The difference in total flow acquisition time between the patients with cirrhosis and the healthy young volunteers was significant (P = .005). The number of acquired cardiac time frames over the cardiac cycle depended on individual heart rates (mean for patients with cirrhosis, 16.7 time frames ± 2.9; mean for healthy age-matched control subjects, 17.3 time frames ± 2.7; mean for healthy young volunteers, 19.6 time frames ± 3.1).

Three-dimensional Visualization of Portal Venous Hemodynamics

Three-dimensional streamlines and particle traces helped visualization of the hemodynamics of nearly the entire portal venous system, with good

Figure 2

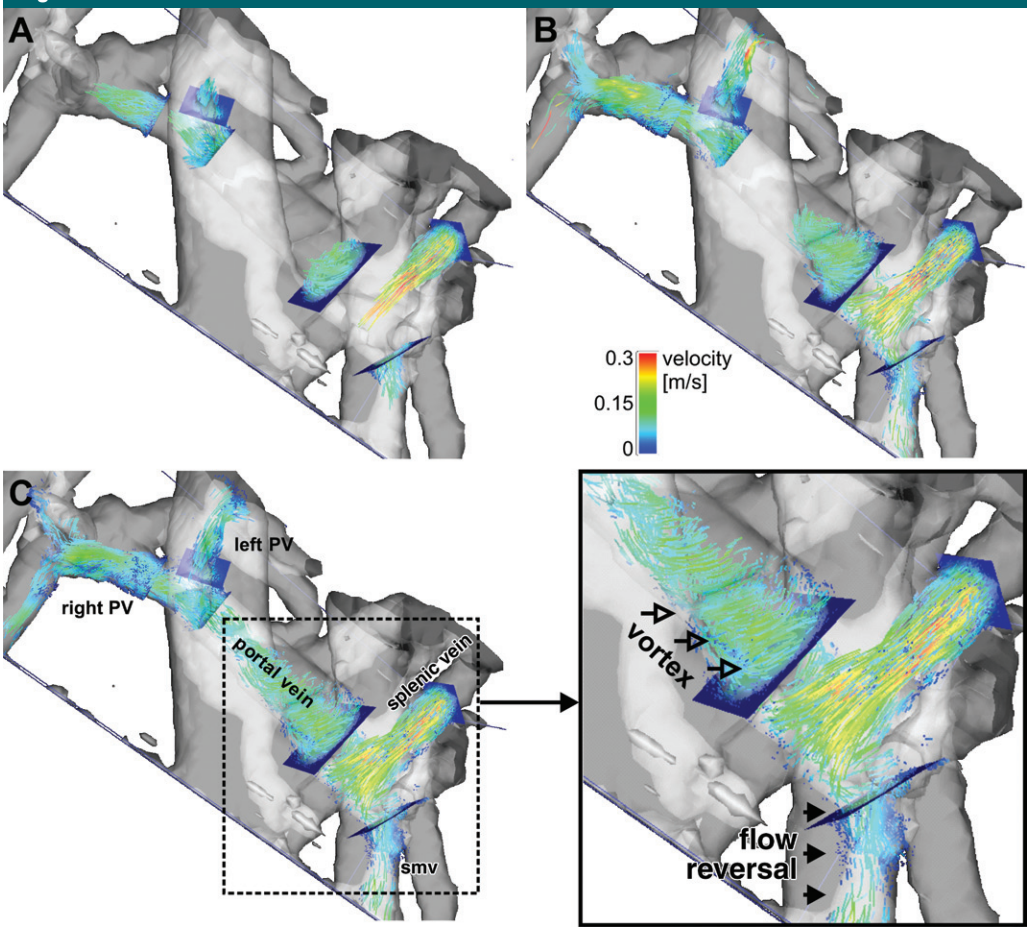

Figure 2: Portal venous system visualized with time-resolved 3D particle traces (proceeding from *A* to *C*) in a 65-year-old female patient with liver cirrhosis (Child-Pugh class A). Bottom right, shows detail zoom of time step *C*. Blood flow originating from the splenic vein develops into retrograde flow in the superior mesenteric vein (flow reversal) and a vortex in the splenic-mesenteric confluence (vortex). Keys are the same as on Figure 1.

image quality, in all 61 subjects (Table 2). Both readers reported clear visibility of extrahepatic vessels, except the splenic vein in one case. For the intrahepatic vessels, visualization of the left intrahepatic branch was limited, with complete visibility (grade 2) of 87% reported by reader A (Z.S.) and 89% reported by reader B (Z.C.) (Table 2). We observed an overall consensus of 93% between the two readers. The Cohen κ coefficient for interobserver variability was 0.70, which represented substantial agreement.

Leakage of calculated streamlines into adjacent vessels was observed in 51 of 61 (84%) subjects (reader A) and 52 of 61 (85%) subjects (reader B), whereas particle traces revealed leakage in 31 of 61 (51%) subjects (reader A) and 29 of 61 (48%) subjects (reader B) (Table 2).

Nineteen patients with cirrhosis demonstrated physiologic portal vein flow hemodynamics in the extrahepatic part, with inflow in the splenic-mesenteric confluence from the splenic and superior mesenteric veins, while six of them showed a reopening of the umbilical vein with inflow from the left intrahepatic portal vein branch (Fig 1). All these findings were detected by using 4D MR imaging and Doppler US, respectively. One patient demonstrated retrograde blood flow in the superior mesenteric vein originating from the splenic vein. The remaining flow from the splenic vein went into the splenic-mesenteric confluence, with a vortex in the inflow (Fig 2). This patient's complex portal venous hemodynamic abnormality was only visible at MR imaging, while we were not able to clearly assess the superior mesenteric vein, including the blood flow direction within the vessel, with US. Physiologic flow patterns were observed in all healthy age-matched control subjects and healthy young volunteers.

Quantification of Portal Venous Hemodynamics

Results of velocity, flow, and area quantification for all groups are summarized in Table 3 and Figure 3. Flow-sensitive 4D MR imaging revealed significantly lower values for maximum (0.15–0.23 m/sec) ($P < .001$) and mean velocities (0.06–0.09 m/sec) ($P < .001$) compared with values for maximum and mean velocities revealed with Doppler US (0.18–0.35 m/sec and 0.08–0.15 m/sec, respectively). Correlations between MR and US were moderate but significant (r = 0.31–0.64, P = .001–.017) on almost all planes, except for maximum velocities in the splenic vein and mean velocities in the left intrahepatic branch. Flow volume correlated moderately but significantly (r = 0.27–0.56, P = .001–.039) on all planes between 4D MR imaging (0.25–0.68 L/min) and US (0.31–0.92 L/min), with no significant difference in the splenic (P = .59) and superior mesenteric (P = .062) veins but with a significant difference in the splenic-mesenteric confluence and intrahepatic branches ($P < .001$ to P = .045). Vessel area quantification in all groups revealed significantly higher values ($P < .001$) in MR imaging (83–163 cm^2) compared with Doppler US (26–54 cm^2), with moderate but significant correlations (r = 0.27–0.54, P = .001–.044).

Compared with healthy age-matched control subjects and healthy young volunteers, patients with cirrhosis demonstrated significantly lower mean velocities in the superior mesenteric vein (38% in MR, 27% in Doppler US; P = .003–.012), whereas flow volumes in the splenic vein were significantly higher (64% in MR, 85% in Doppler US; $P <$ .001 to P = .009). Analysis revealed a significant increase in vessel lumen area of the splenic vein and left intrahepatic portal vein branch with both modalities (P = .002–.048) (Table 3, Fig 3) between patients with cirrhosis and healthy age-matched control subjects.

Clinical demographic analysis of all three cohorts revealed no relevant correlation for portal venous flow parameters, including velocities, flow volume, and area. Subanalysis of quantitative measurements and MELD scores, including maximum and mean velocities, flow volume, and area, revealed no relevant correlation in 4D MR imaging measurements (mean correlation, r = 0.147 ± 0.140; range, 0.024–0.475) or Doppler US measurements (mean correlation, r = 0.266 ± 0.132; range, 0.009–0.512). A significant correlation was detected in only the left intrahepatic portal vein branch in MR imaging for mean velocity (r = 0.475, P = .046) and in Doppler US for maximum velocity (r = 0.512, P = .025) and mean velocity (r = 0.496, P = .031).

Discussion

Flow-sensitive 4D MR imaging depicted 3D portal venous blood flow in patients with liver cirrhosis, with good image quality and low observer variability. Similar to Doppler US, the portal venous system's complex vascular geometry was visualized, including abnormal flow patterns involving a reopening of the umbilical vein in six patients. With only MR imaging were complex and abnormal blood flow successfully visualized in one patient's extrahepatic vessels, presenting retrograde flow in the superior mesenteric vein originating from the splenic vein. No reference standard was available to confirm our findings in this case, as these findings could not be confirmed with Doppler US. In addition, quantitative flow analysis demonstrated a good correlation between the quantitative evaluation of regional hemodynamic parameters and the Doppler US reference standard.

To clinically evaluate chronic liver disease resulting in fibrosis and cirrhosis, serum-marker levels are tested (30) or liver stiffness is measured through US-based transient elastography (31). Established MR-based diagnostic liver imaging techniques include MR imaging morphology diffusion (32) and perfusion techniques (13), MR elastography (33), and MR spectroscopy (34). However, the assessment of portal venous flow hemodynamics has attracted growing attention in recent studies (16,22).

Following a recently reported pilot study (21), we applied flow-sensitive 4D MR imaging of portal venous hemodynamics in a larger cohort of patients with liver cirrhosis. In contrast to previous studies that were based on quantitative flow measurements (7,15,16,35), we evaluated not just portal venous hemodynamics but the flow in the extrahepatic vessels as well, including the superior mesenteric and splenic veins and intrahepatic vessels with the right and left intrahepatic portal vein branches. Almost all extrahepatic vessels were well visualized with good quality, with some limitations in the left intrahepatic branches.

One limitation associated with this imaging protocol was our finding that streamlines and particle traces consistently revealed leakage into adjacent vessels, most likely caused by insufficient spatial resolution, which did not allow us to completely separate adjacent vessels. In addition, long image times of 15–20 minutes and data acquisition during free breathing may have induced additional blurring by organ motion caused by imperfect respiration control. Improvements in spatial resolution and respiration control and their effects on visualization quality should thus be explored in future studies. Newly described imaging techniques that are based on undersampling along spatial and temporal dimensions may help to substantially accelerate flow-sensitive MR imaging and permit the acquisition of data with higher spatial resolution and/or reduced total image times (36,37).

In addition to 3D flow visualization, we also analyzed flow quantitatively, which revealed moderate but significant correlations between 4D MR imaging and Doppler US in most of the hemodynamic parameters. Blood flow velocities were quantified by a single reader, representing a limitation of our study, which may have led to a systematic evaluation error. We observed that underestimation of the maximum and mean velocities by 35% and 38% occurred with MR imaging compared with Doppler US, a finding that supports data in the study of Harloff et al (38), who reported

Table 3

Summary of 4D MR Imaging and Doppler US Flow Quantification Results in Five Analysis Planes in All Three Cohorts

Parameter, Imaging Method, and Structure	Group A	Group B	Group C	*P* Value		
				Group A vs Group B	Group A vs Group C	Group B vs Group C
Maximum velocity (m/sec)						
4D MR imaging						
Superior mesenteric vein	0.14 ± 0.04	0.17 ± 0.04	0.2 ± 0.09	.064*	.02†	.308*
Splenic vein	0.21 ± 0.05	0.21 ± 0.06	0.21 ± 0.05	.737‡	.753‡	.949‡
Splenic-mesenteric confluence	0.20 ± 0.06	0.22 ± 0.04	0.26 ± 0.09	.089*	.005†	.154*
Right portal vein branch	0.18 ± 0.04	0.17 ± 0.05	0.19 ± 0.06	.474‡	.475‡	.2‡
Left portal vein branch	0.17 ± 0.05	0.14 ± 0.04	0.14 ± 0.04	.028§	.043§	.759‡
US						
Superior mesenteric vein	0.25 ± 0.09	0.32 ± 0.11	0.36 ± 0.13	.024§	.005§	.387‡
Splenic vein	0.27 ± 0.04	0.26 ± 0.05	0.21 ± 0.04	.171*	<.001†	.003†
Splenic-mesenteric confluence	0.32 ± 0.07	0.36 ± 0.10	0.37 ± 0.10	.693*	.058*	.834*
Right portal vein branch	0.22 ± 0.04	0.24 ± 0.05	0.25 ± 0.05	.231‡	.052‡	.437‡
Left portal vein branch	0.19 ± 0.06	0.17 ± 0.05	0.19 ± 0.06	.297*	.807*	.047*
Mean velocity (m/sec)						
4DMR imaging						
Superior mesenteric vein	0.05 ± 0.03	0.08 ± 0.01	0.08 ± 0.04	.003§	.012§	.779‡
Splenic vein	0.09 ± 0.03	0.09 ± 0.03	0.08 ± 0.02	.765‡	.473‡	.709‡
Splenic-mesenteric confluence	0.08 ± 0.03	0.10 ± 0.02	0.11 ± 0.04	.14‡	.034§	.277‡
Right portal vein branch	0.08 ± 0.03	0.07 ± 0.03	0.08 ± 0.02	.383‡	.585‡	.64‡
Left portal vein branch	0.07 ± 0.03	0.06 ± 0.02	0.05 ± 0.02	.222‡	.001§	.005§
US						
Superior mesenteric vein	0.11 ± 0.03	0.15 ± 0.04	0.15 ± 0.05	.006†	.003†	.948*
Splenic vein	0.12 ± 0.02	0.12 ± 0.03	0.10 ± 0.02	.517‡	.001§	.002§
Splenic-mesenteric confluence	0.14 ± 0.02	0.16 ± 0.04	0.15 ± 0.04	.062‡	.369‡	.367‡
Right portal vein branch	0.11 ± 0.02	0.12 ± 0.03	0.11 ± 0.02	.118*	.772*	.067*
Left portal vein branch	0.08 ± 0.03	0.08 ± 0.02	0.08 ± 0.03	.309‡	.947‡	.29‡
Flow volume (L/min)						
4D MR imaging						
Superior mesenteric vein	0.29 ± 0.15	0.31 ± 0.11	0.36 ± 0.48	>.99*	.341*	.21*
Splenic vein	0.46 ± 0.26	0.28 ± 0.15	0.24 ± 0.12	.009§	.001§	.425‡
Splenic-mesenteric confluence	0.79 ± 0.32	0.64 ± 0.19	0.67 ± 0.54	.11*	.043†	.396*
Right portal vein branch	0.42 ± 0.19	0.38 ± 0.21	0.5 ± 0.44	.568‡	.48‡	.294‡
Left portal vein branch	0.41 ± 0.31	0.21 ± 0.13	0.18 ± 0.19	.005†	<.001†	.12*
US						
Superior mesenteric vein	0.40 ± 0.31	0.35 ± 0.23	0.38 ± 0.17	.57*	.754*	.279*
Splenic vein	0.5 ± 0.41	0.27 ± 0.09	0.24 ± 0.08	.002†	<.001†	.225*
Splenic-mesenteric confluence	1.02 ± 0.54	0.82 ± 0.34	0.90 ± 0.35	.168‡	.371‡	.5‡
Right portal vein branch	0.52 ± 0.22	0.51 ± 0.2	0.53 ± 0.15	.895‡	.794‡	.647‡
Left portal vein branch	0.43 ± 0.41	0.21 ± 0.10	0.29 ± 0.14	.01†	.297*	.044†
Vessel area (cm^2)						
4D MR imaging						
Superior mesenteric vein	126.7 ± 78.8	93.3 ± 28.6	82.9 ± 27.5	.043†	.001†	.175*
Splenic vein	119.6 ± 73.5	67.9 ± 25.9	61.9 ± 21.6	.009†	.002†	.375*
Splenic-mesenteric confluence	208.4 ± 77.0	153.0 ± 35.4	129.6 ± 51.6	.007§	.001§	.1‡
Right portal vein branch	112.4 ± 52.9	113.0 ± 43.7	126.1 ± 51.6	.967‡	.412‡	.387‡
Left portal vein branch	114.3 ± 14.5	71.3 ± 31.0	71.1 ± 29.1	.019†	.021†	.876*

Table 3 (continues)

Table 3 (continued)

Summary of 4D MR Imaging and Doppler US Flow Quantification Results in Five Analysis Planes in All Three Cohorts

Parameter, Imaging Method, and Structure	Group A	Group B	Group C	*P* Value		
				Group A vs Group B	Group A vs Group C	Group B vs Group C
US						
Superior mesenteric vein	31.5 ± 17.7	22.1 ± 12.6	24.0 ± 11.4	.059‡	.114‡	.603‡
Splenic vein	36.6 ± 29.5	20.6 ± 6.1	23.4 ± 7.1	.002†	.02†	.279*
Splenic-mesenteric confluence	64.0 ± 31.6	45.4 ± 16.3	51.6 ± 12.3	.026§	.113‡	.177‡
Right portal vein branch	44.9 ± 17.6	41.8 ± 14.0	46.2 ± 14.7	.544‡	.799‡	.331‡
Left portal vein branch	42.6 ± 24.3	25.9 ± 11.7	30.9 ± 9.15	.011§	.048§	.12‡

Note.—Group A = patients with cirrhosis ($n = 20$), group B = healthy age-matched control subjects ($n = 20$), and group C = healthy young volunteers ($n = 21$). All measurements were taken after overnight fasting.

* Mann-Whitney test.

† Mann-Whitney test; significant difference with $P < .05$.

‡ *t* Test.

§ *t* Test; significant difference with $P < .05$.

Figure 3

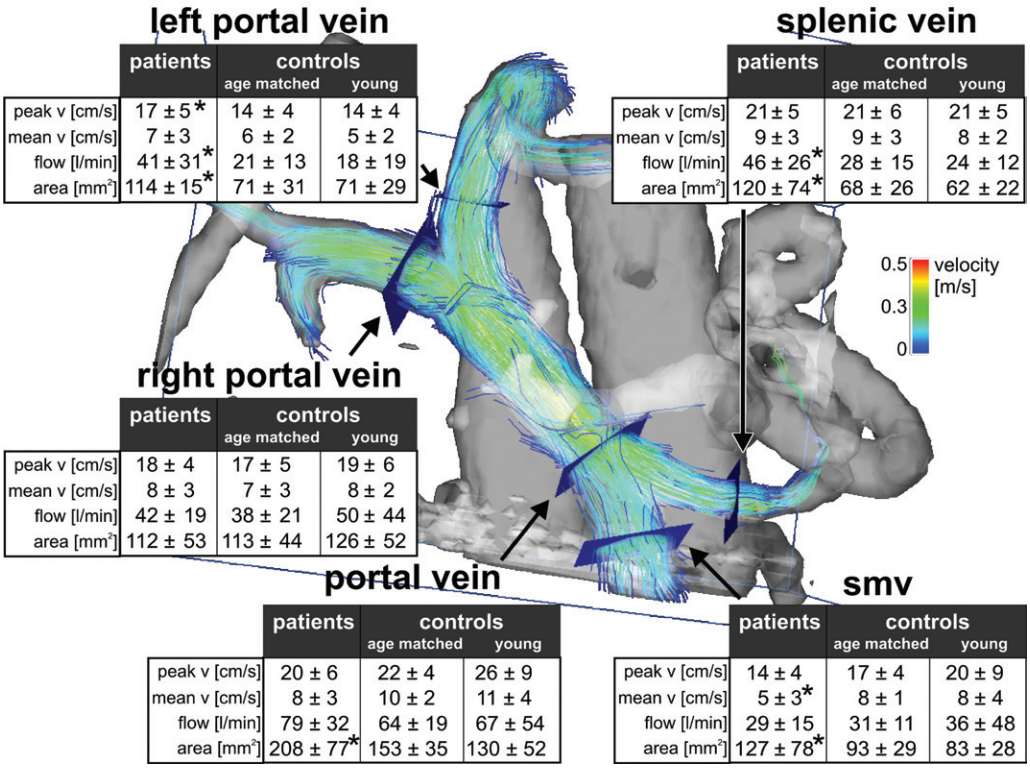

Figure 3: Streamline visualization of portal venous flow in a 59-year-old female patient with liver cirrhosis (Child-Pugh class A) with a reopened umbilical vein and flow over the left portal vein branch. The tables summarize MR-based velocity and flow quantification results of all 61 study subjects, and the data are the mean ± standard deviation. ★ = Significant differences ($P \leq .05$) among patients with cirrhosis *(patients)*, and healthy age-matched control subjects *(age-matched)*. Young healthy volunteers = *young*. Comparison with Doppler US results is provided in Table 3. *mean v* = Mean velocity, *peak v* = peak/maximum velocity, *smv* = superior mesenteric vein.

4D MR imaging underestimations of 31%–39% compared with US measurements of blood-flow velocities in the carotid bifurcation. Nanashima et al (35) observed that underestimation of mean flow velocities in the portal vein by 19.2% occurred with MR imaging compared with Doppler US. The maximum (22.7 cm/sec ± 7.1) and mean (9.6 cm/sec ± 3.1) velocities of MR imaging in our study were slightly lower than those in previous MR studies (ie, Yzet et al [16], with a maximum velocity of 28.2 cm/sec ± 8.8; Lycklama à Nijeholt et al [15] and Nanashima et al [35], with a mean velocity of 10.8 cm/sec ± 1.6 to 13.5 cm/sec ± 3.7). With MR imaging, one may tend to underestimate velocity because velocity data are acquired over several cardiac cycles, which yields average velocity-time courses, but one cannot measure cycle-to-cycle velocity variations or short-term fluctuations. Doppler US represents real-time velocity data. Thus, velocity values in MR imaging may be underestimated because of velocity averaging and the partial volume effects associated with the lower spatial resolution of MR imaging compared with Doppler US.

In our study, MR imaging flow volume measurements revealed lower values (mean, 0.7 L/min ± 0.4) than those in the literature (between 1.0 and 1.3 L/min) (15,16,39). In contrast, published Doppler US measurements reveal a wide range (between 0.3 and 1.3 L/min) of flow volumes (40,41). One reason for alterations in portal venous flow velocities and flow volume might be the influence of ingestion, resulting in postprandial hemodynamic changes. A study (42) in which researchers investigated postprandial hyperemia in patients with liver cirrhosis revealed a mean increase in portal blood flow velocity of 28.6% and an increase in portal blood flow of 37.5%. A recent study (21) showed no significant differences in peak velocity measurements among 4D MR imaging, 2D phase-contrast imaging, and Doppler US; however, lumen area measurements of the portal vein were significantly higher with 4D MR imaging than with Doppler US. Results of a further study (43) suggest that small errors in velocity can result in large errors in flow caused by integration over the region of interest and over time, resulting in large differences in total flow. We therefore speculate that the differences in MR imaging and US flow measurements are mostly related to partial volume effects.

Concordant with our findings, investigators in earlier studies report larger portal vein areas when assessed with MR imaging compared with Doppler US (15,35). A potential source of dissenting results between MR imaging and Doppler US measurements of portal vein area size may be measurement site differences, representing a limitation of our study. We assume that Doppler US measurements tend to be rather unreliable because of difficulties in Doppler insonation angulation and location during diameter measurement, compromising the precise determination of vessel diameter while reflecting strong interobserver dependency (44).

Researchers in previous studies (6,40) described significantly lower flow velocity and flow volume in patients with cirrhosis and at different stages of liver disease compared with healthy volunteers. However, subanalysis of quantitative measurements and MELD scores revealed no relevant correlation between disease severity and flow changes in our patient cohort in the 4D MR imaging and Doppler US measurements. The expected changes in velocities and flow volume were restricted to isolated vessels in the portal venous system. Instead, MR imaging assessment of the vessel areas in patients with cirrhosis showed almost all vessels yielding significantly higher values, indicating early changes in vascular geometry.

Our study had several limitations: First, our patients form a rather homogeneous cohort, in that most had Child-Pugh class A stage of liver cirrhosis and few had Child-Pugh class B or C stages; this revealed the onset of venous flow alterations in patients with cirrhosis and a shortage of more substantial differences between patients with cirrhosis and healthy age-matched control subjects. In their study, Gaiani et al (45) described an overall prevalence of spontaneous hepatofugal portal flow in 8.3% of subjects in a cohort of 228 patients with liver cirrhosis and portal hypertension. This finding was more prevalent in patients with higher Child-Pugh classes (eg, Child-Pugh class C [15.4%] and Child-Pugh class B [12.5%]) compared with patients classified with Child-Pugh class A (2.7%) cirrhosis. Because our patient cohort was made up largely of patients with Child-Pugh class A stage (ie, mild) cirrhosis, we anticipated a low incidence of hepatofugal portal flow in our cohort (one of 20 patients). Furthermore, portal vein flow velocities decrease in advanced Child-Pugh classes (6). Moreover, the heterogeneity of etiologies for cirrhosis in our patient cohort might introduce differences in observed portal venous flow patterns. For example, patients with alcohol-induced cirrhosis compared with virus-induced cirrhosis might have more distinctive sinusoidal distortion and higher sinusoidal resistance with consecutive slower portal flow (46) and, thus, a higher frequency of a visible paraumbilical vein in alcoholic liver cirrhosis (47). Additional studies with larger patient cohorts consisting of each Child-Pugh classes and different etiologies for liver cirrhosis are necessary to evaluate potential correlations between disease severities and altered 4D MR imaging–measured portal venous flow in patients with cirrhosis. Furthermore, our data evaluation and acquisition only focused on portal venous blood flow with low velocities; they thus provide no information on hepatic arterial flow. To evaluate the interaction and context within the splanchnic system, one must assess arterial flow, representing the blood supply, as well as portal venous flow, representing the blood flow outcome. Additional studies are needed to evaluate these interactions between arterial and portal venous hemodynamics within the splanchnic system in well-defined clinical problems (eg, portal venous thrombosis, anastomotic stenosis after liver transplantation, after transarterial chemoembolization or transjugular intrahepatic portosystemic shunt implantation). In addition, high-quality reference standards such as invasive

catheter measurements (flow, pressure) may be needed to improve the validation of flow-sensitive 4D MR imaging. Another feature of flow-sensitive 4D MR imaging may be to estimate portal venous pressure. While it is not possible to derive absolute pressure from flow-sensitive MR data, several previous studies have shown that it is possible to calculate pressure difference maps that are based on the Navier-Stokes Equations (48). Measured three-directional velocities and assumptions of blood viscosity and density can be used to estimate pressure gradients inside connected vascular segments. Future studies are warranted to evaluate the possibility of deriving portal venous pressure difference maps and to assess their potential for characterizing liver disease.

In conclusion, flow-sensitive 4D MR imaging with broad volumetric coverage enables us to retrospectively and nearly comprehensively visualize flow hemodynamics in the portal venous system of patients with liver cirrhosis, with good image quality and low interobserver variability. Flow quantification revealed a significant correlation between 4D MR imaging and Doppler US in maximum and mean velocities, flow volume, and vessel area. Granted, our claim is premature because of the small amount of data presented in this study, but we nevertheless believe that 4D flow-sensitive MR imaging may prove to be useful for evaluating patients with cirrhosis. It may eventually give us insights into the pathophysiologic features of cirrhosis that are not accessible with currently available techniques and become a more sensitive and specific means of classifying disease severity than methods currently in use. Flow-sensitive 4D MR imaging may be an alternative to Doppler US and may represent a noninvasive, standardized, and investigator-independent technique, supplying information about portal venous hemodynamics and pathologic changes in flow characteristics in patients with liver cirrhosis.

Disclosures of Potential Conflicts of Interest: **Z.S.** No potential conflicts of interest to disclose. **Z.C.** No potential conflicts of interest to disclose. **P.D.** No potential conflicts of interest to disclose. **W.E.** No potential conflicts of interest to disclose. **P.B.** No potential conflicts of interest to disclose. **W.K.** No potential conflicts of interest to disclose. **Z.A.Z.** No potential conflicts of interest to disclose. **F.K.** No potential conflicts of interest to disclose. **M.L.** No potential conflicts of interest to disclose. **M.M.** No potential conflicts of interest to disclose.

References

1. Groszmann RJ. Hyperdynamic circulation of liver disease 40 years later: pathophysiology and clinical consequences. Hepatology 1994;20(5):1359–1363.
2. Bosch J, García-Pagán JC. Complications of cirrhosis. I. Portal hypertension. J Hepatol 2000;32(1, suppl):141–156.
3. Lautt WW. Mechanism and role of intrinsic regulation of hepatic arterial blood flow: hepatic arterial buffer response. Am J Physiol 1985;249(5 pt 1):G549–G556.
4. Abraldes JG, Tarantino I, Turnes J, Garcia-Pagan JC, Rodés J, Bosch J. Hemodynamic response to pharmacological treatment of portal hypertension and long-term prognosis of cirrhosis. Hepatology 2003;37(4):902–908.
5. Albillos A, Bañares R, González M, et al. Value of the hepatic venous pressure gradient to monitor drug therapy for portal hypertension: a meta-analysis. Am J Gastroenterol 2007;102(5):1116–1126.
6. Taourel P, Blanc P, Dauzat M, et al. Doppler study of mesenteric, hepatic, and portal circulation in alcoholic cirrhosis: relationship between quantitative Doppler measurements and the severity of portal hypertension and hepatic failure. Hepatology 1998;28(4):932–936.
7. Zekanovic D, Ljubicic N, Boban M, et al. Doppler ultrasound of hepatic and system hemodynamics in patients with alcoholic liver cirrhosis. Dig Dis Sci 2010;55(2):458–466.
8. Kok T, van der Jagt EJ, Haagsma EB, Bijleveld CM, Jansen PL, Boeve WJ. The value of Doppler ultrasound in cirrhosis and portal hypertension. Scand J Gastroenterol Suppl 1999;230:82–88.
9. Takayasu K, Yoshie K, Muramatsu Y, et al. Haemodynamic changes in non-alcoholic (viral) liver cirrhosis studied by computed tomography (CT) arterial portography and CT arteriography. J Gastroenterol Hepatol 1999;14(9):908–914.
10. Van Beers BE, Leconte I, Materne R, Smith AM, Jamart J, Horsmans Y. Hepatic perfusion parameters in chronic liver disease: dynamic CT measurements correlated with disease severity. AJR Am J Roentgenol 2001;176(3):667–673.
11. Gomi T, Nagamoto M, Hasegawa M, et al. Are there any differences in acute adverse reactions among five low-osmolar nonionic iodinated contrast media? Eur Radiol 2010;20(7):1631–1635.
12. De Cecco CN, Buffa V, Fedeli S, et al. Dual energy CT (DECT) of the liver: conventional versus virtual unenhanced images. Eur Radiol 2010;20(12):2870–2875.
13. Annet L, Materne R, Danse E, Jamart J, Horsmans Y, Van Beers BE. Hepatic flow parameters measured with MR imaging and Doppler US: correlations with degree of cirrhosis and portal hypertension. Radiology 2003;229(2):409–414.
14. Barthelmes D, Parviainen I, Vainio P, et al. Assessment of splanchnic blood flow using magnetic resonance imaging. Eur J Gastroenterol Hepatol 2009;21(6):693–700.
15. Lycklama à Nijeholt GJ, Burggraaf K, Wasser MN, et al. Variability of splanchnic blood flow measurements using MR velocity mapping under fasting and post-prandial conditions: comparison with echo-Doppler. J Hepatol 1997;26(2):298–304.
16. Yzet T, Bouzerar R, Allart JD, et al. Hepatic vascular flow measurements by phase contrast MRI and Doppler echography: a comparative and reproducibility study. J Magn Reson Imaging 2010;31(3):579–588.
17. Buonocore MH. Visualizing blood flow patterns using streamlines, arrows, and particle paths. Magn Reson Med 1998;40(2):210–226.
18. Kilner PJ, Yang GZ, Wilkes AJ, Mohiaddin RH, Firmin DN, Yacoub MH. Asymmetric redirection of flow through the heart. Nature 2000;404(6779):759–761.
19. Kozerke S, Hasenkam JM, Pedersen EM, Boesiger P. Visualization of flow patterns distal to aortic valve prostheses in humans using a fast approach for cine 3D velocity mapping. J Magn Reson Imaging 2001;13(5):690–698.
20. Frydrychowicz A, Arnold R, Harloff A, et al. Images in cardiovascular medicine: in vivo 3-dimensional flow connectivity mapping after extracardiac total cavopulmonary connection. Circulation 2008;118(2):e16–e17. doi:10.1161/CIRCULATIONAHA.107.761304. Accessed December 11, 2010.
21. Stankovic Z, Frydrychowicz A, Csatari Z, et al. MR-based visualization and quantification of three-dimensional flow character-

istics in the portal venous system. J Magn Reson Imaging 2010;32(2):466–475.

22. Verma RW, Johnson K, Landgraf B, et al. Hemodynamics of portal hypertension with 4D radial phase contrast imaging: feasibility at 3.0T [abstr]. In: Proceedings of the Eighteenth Meeting of the International Society for Magnetic Resonance in Medicine. Berkeley, Calif: International Society for Magnetic Resonance in Medicine, 2010; 561.

23. Pugh RN, Murray-Lyon IM, Dawson JL, Pietroni MC, Williams R. Transection of the oesophagus for bleeding oesophageal varices. Br J Surg 1973;60(8):646–649.

24. Markl M, Harloff A, Bley TA, et al. Time-resolved 3D MR velocity mapping at 3T: improved navigator-gated assessment of vascular anatomy and blood flow. J Magn Reson Imaging 2007;25(4):824–831.

25. Walker PG, Cranney GB, Scheidegger MB, Waseleski G, Pohost GM, Yoganathan AP. Semiautomated method for noise reduction and background phase error correction in MR phase velocity data. J Magn Reson Imaging 1993;3(3):521–530.

26. Bernstein MA, Zhou XJ, Polzin JA, et al. Concomitant gradient terms in phase contrast MR: analysis and correction. Magn Reson Med 1998;39(2):300–308.

27. Bock J, Kreher BW, Hennig J, Markl M. Optimized pre-processing of time-resolved 2D and 3D phase contrast MRI data [abstr]. In: Proceedings of the Fifteenth Meeting of the International Society for Magnetic Resonance in Medicine. Berkeley, Calif: International Society for Magnetic Resonance in Medicine, 2007; 3138.

28. Bock J, Frydrychowicz A, Stalder AF, et al. 4D phase contrast MRI at 3 T: effect of standard and blood-pool contrast agents on SNR, PC-MRA, and blood flow visualization. Magn Reson Med 2010;63(2):330–338.

29. Landis JR, Koch GG. The measurement of observer agreement for categorical data. Biometrics 1977;33(1):159–174.

30. Imbert-Bismut F, Ratziu V, Pieroni L, et al. Biochemical markers of liver fibrosis in patients with hepatitis C virus infection: a prospective study. Lancet 2001;357(9262):1069–1075.

31. Castera L, Forns X, Alberti A. Non-invasive evaluation of liver fibrosis using transient elastography. J Hepatol 2008;48(5):835–847.

32. Taouli B, Koh DM. Diffusion-weighted MR imaging of the liver. Radiology 2010;254(1):47–66.

33. Muthupillai R, Lomas DJ, Rossman PJ, Greenleaf JF, Manduca A, Ehman RL. Magnetic resonance elastography by direct visualization of propagating acoustic strain waves. Science 1995;269(5232):1854–1857.

34. Longo R, Ricci C, Masutti F, et al. Fatty infiltration of the liver. Quantification by 1H localized magnetic resonance spectroscopy and comparison with computed tomography. Invest Radiol 1993;28(4):297–302.

35. Nanashima A, Shibasaki S, Sakamoto I, et al. Clinical evaluation of magnetic resonance imaging flowmetry of portal and hepatic veins in patients following hepatectomy. Liver Int 2006;26(5):587–594.

36. Jung B, Honal M, Ullmann P, Hennig J, Markl M. Highly k-t-space-accelerated phase-contrast MRI. Magn Reson Med 2008;60(5):1169–1177.

37. Baltes C, Kozerke S, Hansen MS, Pruessmann KP, Tsao J, Boesiger P. Accelerating cine phase-contrast flow measurements using k-t BLAST and k-t SENSE. Magn Reson Med 2005;54(6):1430–1438.

38. Harloff A, Albrecht F, Spreer J, et al. 3D blood flow characteristics in the carotid artery bifurcation assessed by flow-sensitive 4D MRI at 3T. Magn Reson Med 2009;61(1):65–74.

39. Sugano S, Yamamoto K, Sasao K, Watanabe M. Portal venous blood flow while breath-holding after inspiration or expiration and during normal respiration in controls and cirrhotics. J Gastroenterol 1999;34(5):613–618.

40. Tziafalia C, Vlychou M, Tepetes K, Kelekis N, Fezoulidis IV. Echo-Doppler measurements of portal vein and hepatic artery in asymptomatic patients with hepatitis B virus and healthy adults. J Gastrointestin Liver Dis 2006;15(4):343–346.

41. Shi BM, Wang XY, Mu QL, Wu TH, Xu J. Value of portal hemodynamics and hypersplenism in cirrhosis staging. World J Gastroenterol 2005;11(5):708–711.

42. Ozdogan O, Atalay H, Cimsit C, et al. Role of echo Doppler ultrasonography in the evaluation of postprandial hyperemia in cirrhotic patients. World J Gastroenterol 2008;14(2):260–264.

43. Gatehouse PD, Rolf MP, Graves MJ, et al. Flow measurement by cardiovascular magnetic resonance: a multi-centre multi-vendor study of background phase offset errors that can compromise the accuracy of derived regurgitant or shunt flow measurements. J Cardiovasc Magn Reson 2010;12:5.

44. Winkfield B, Aubé C, Burtin P, Calès P. Inter-observer and intra-observer variability in hepatology. Eur J Gastroenterol Hepatol 2003;15(9):959–966.

45. Gaiani S, Bolondi L, Li Bassi S, Zironi G, Siringo S, Barbara L. Prevalence of spontaneous hepatofugal portal flow in liver cirrhosis: clinical and endoscopic correlation in 228 patients. Gastroenterology 1991;100(1):160–167.

46. Bolognesi M, Sacerdoti D, Mescoli C, et al. Different hemodynamic patterns of alcoholic and viral endstage cirrhosis: analysis of explanted liver weight, degree of fibrosis and splanchnic Doppler parameters. Scand J Gastroenterol 2007;42(2):256–262.

47. Chen CH, Wang JH, Lu SN, et al. Comparison of prevalence for paraumbilical vein patency in patients with viral and alcoholic liver cirrhosis. Am J Gastroenterol 2002;97(9):2415–2418.

48. Bock J, Frydrychowicz A, Lorenz R, et al. In vivo noninvasive 4D pressure difference mapping in the human aorta: phantom comparison and application in healthy volunteers and patients. Magn Reson Med 2011;66(4):1079–1088.